Catalytic Supercritical Water Oxidation: Stability of Cr_2O_3 Catalyst

Sudhir N. V. K. Aki, Zhong-Yi Ding, and Martin A. Abraham
Dept. of Chemical Engineering, The University of Tulsa, Tulsa, OK 74104

Supercritical water oxidation has become a well-known treatment technology for conversion of aqueous wastes. By introducing a catalyst, higher conversion and selectivity to carbon dioxide can be achieved at a lower temperature and at shorter residence times. The stability of chromium oxide in supercritical water was studied to determine the feasibility of using catalysts during supercritical water oxidation. Various process variables, including oxygen and water concentrations, fluid flow rate, and temperature were found to affect the reactivity of the chromium oxide catalyst. Under these conditions, chromium was present in the reactor effluent as chromic acid, H_2CrO_4. The visual observation of the catalyst after the completion of the experiments suggested that a reaction front moved along the length of the reactor. A rate expression, based on Langmuir–Hinshelwood kinetics, with dissociative chemisorption of oxygen on a hydrated chromium oxide surface, was proposed. The model, developed based on this rate expression and the continuity equation for the fluid phase, was consistent with the experimental results.

Introduction

Supercritical water oxidation (SCWO) has been developed to destroy organic compounds by oxidation in water at temperatures and pressures above its critical point, which is approximately 374°C and 22.1 MPa (218 atm). This process is generally conducted at 400°C to 650°C and about 24 to 35 MPa, and is capable of achieving a high destruction efficiency. There is no formation of NO_x or SO_2, and *in-situ* neutralization of the produced acid gases can be achieved (Barner et al., 1992). Any inorganic salts that are formed precipitate in the reaction medium and can be separated in the reactor vessel.

Supercritical fluids assume gaslike transport properties and liquidlike densities; the physical properties can be controlled by changes in temperature and/or pressure. For example, the dielectric constant of water at temperatures and pressures of interest in SCWO drops to values similar to nonpolar organic compounds at ambient conditions (Quist, 1970), the ion product decreases below 10^{-20} $(mol/kg)^2$ (Marshall and Franck, 1981), and hydrogen bonding is notably less extensive (Franck, 1970). Thus gases and hydrocarbons are completely soluble in supercritical water (Japas and Franck, 1985), whereas inorganic salts that are soluble in subcritical water become insoluble in supercritical water (Dell'Orco et al., 1992).

Several laboratory-scale SCWO reactors (both batch and flow systems) have been constructed and operated. Most of the research conducted with these reactors involves homogeneous oxidation of organic compounds that closely model certain hazardous wastes; kinetic parameters were often measured (Barner et al., 1992; Bramlette et al., 1980; Helling and Tester, 1986). Simple model compounds were selected in an effort to understand the reaction mechanism occurring at these conditions with the hope of extending the results to develop SCWO as a hazardous waste treatment process.

To obtain a destruction efficiency in excess of 99.99% for the organic species, reaction temperatures greater than 600°C are generally required. As an alternative, a catalyst can be used and the reaction can be performed at a lower temperature. Previous experiments in our laboratory have revealed that MnO_2, V_2O_5, and Cr_2O_3 catalysts can be used to enhance the reactant conversion and the yield to carbon dioxide or can affect the selectivity to partial oxidation products (Ding et al., 1994; Jin et al., 1992). Frisch (1992) found that acetic acid destruction can be increased from less than 40% to greater than 95% by adding a catalyst at 400°C and a residence time of 5 minutes.

In the development of a process based on catalytic supercritical water oxidation (CSCWO), one significant issue that must be resolved is the stability of the catalyst. A potential catalyst can be selected based upon solubility data for the catalyst in high-temperature, high-pressure water. Even though no quantitative data exist for the solubility of Cr_2O_3 in high-pressure, high-temperature water (Blesa and Maroto, 1986), data exist for the solubility of various metal oxides in water, including nickel oxide (Tremaine and LeBlanc, 1980b) and cupric oxide (Hearn et al., 1969), as well as oxide minerals such as quartz (Morey and Hesselgesser, 1951) and magnetite (Tremaine and LeBlanc, 1980a; Holser and Schneer, 1961; I-Ming and Eugster, 1977). The solubility of inorganic compounds in subcritical and supercritical water was reviewed by Martynova (1964).

The stability of a heterogeneous catalyst is not unlike the issue of reactor corrosion, which was found to be important during SCWO. For example, Barner et al. (1992) conducted corrosion experiments in a continuous-flow bench scale reactor by exposing long narrow strip specimens of various alloys including Inconel 625, and Hastelloy C22 and C276 to supercritical water. Higher corrosion rates than are typically acceptable in the design of chemical process plants were found. Although little quantitative data exist for corrosion during SCWO, substantial data exist for SS316 (Robertson, 1989; Otsuka and Fujikawa, 1991), Inconel 625 (McIntyre et al., 1978; Copson and Berry, 1960), and Hastelloy C276 (Postlethwaite et al., 1988) in high-temperature and high-pressure deoxygenated water, a system important in the power industry. The stability of these materials depends upon the formation of stable metal oxides at the interface consisting of Cr_2O_3 and other metal oxides. Also, significant increase in the corrosion rate of Inconel 600 resulted from an increase in the concentration of the dissolved oxygen in water (McIntyre et al., 1979). This is due to the increased solubility of chromium ion with increased oxygen concentration.

Because of our interest in CSCWO and the relevance to corrosion during SCWO, an experimental facility was constructed to study the stability of metal oxides during CSCWO. The objective of this work was to study the effect of oxygen concentration, temperature, and fluid flow rate on the reaction between Cr_2O_3 and supercritical water. In addition, the effect of added organic compounds on the reaction was investigated. This work impacts our understanding of corrosion and discusses the feasibility of using catalysts during SCWO.

Experimental

A schematic diagram of the experimental apparatus is shown in Figure 1, and can be divided into four sections, namely, feed and preheaters, main reactor section, gas separator, and finally sample collection units.

An LDC Analytical 2396-31-89 series metering pump was used to deliver water at the required flow rates and operating pressure. Millipore, double distilled, and deionized water was used. During all runs, the water was deoxygenated by bubbling nitrogen through the water feed tank overnight and

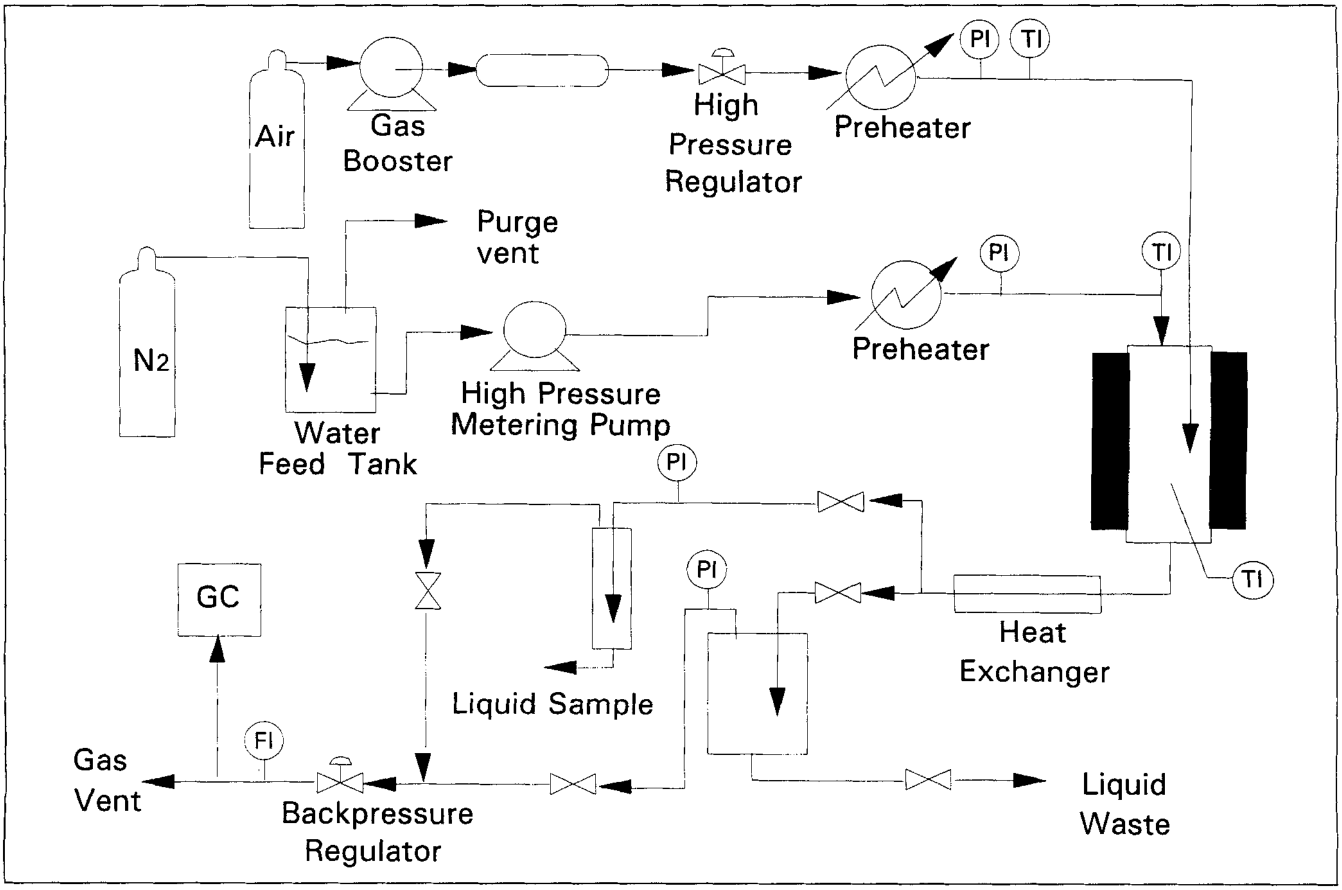

Figure 1. Experimental system.

during the experiment. This eliminated the possibility of oxygen dissolved in water from taking part in the reaction.

A Haskel air-driven gas booster compressed the gas to the required operating pressure. Three different gas mixtures, consisting of 21, 10 or 1% oxygen in nitrogen were used as the gas feed. The use of several gas concentrations in the feed allowed substantial variation in the oxygen concentration inside the reactor.

An Eldex AS-30-S series metering pump was used to pump any organic species (not shown in Figure 1). The organic feed was mixed with the water before entering the reactor in a high-pressure mixing tee. The organic species was introduced only after attaining the desired operating conditions; prior to that, pure water was fed to the reactor. After the experiment was completed, the organic feed pump and the feed line were washed with water by shifting the three-way Teflon valve to water. For the experiments on the effect of the pure water and oxygen on solubility, the organic feed line was disconnected and the tee was replaced with a union.

The water and the gas were fed to the reactor through separate heating units, each consisting of a tube furnace and a temperature controller. An HiP MS-17 Microreactor (2.54 cm OD, 1.27 cm ID, and 25.4 cm long), constructed of Hastelloy C-276 was used as the reactor. An electric furnace was used to maintain the reactor at the required temperature. The temperatures at the reactor inlet and inside the reactor were measured with type-K thermocouples.

The reactor was packed with 22.4 g of low surface area sintered α-alumina and 9.26 g of Cr_2O_3 supported on γ-Al_2O_3 (which contains 12% Cr as Cr_2O_3) having a surface area of 62 m^2/g. All particles were crushed to an average particle size of approximately 0.5 mm. The catalyst bed was supported on a 20-μm Hastelloy C-276 filter. Atomic absorption analysis revealed that the alumina was stable under all reaction conditions.

The effluent from the reactor was cooled using a single pass tube in tube heat exchanger and was separated into gas and liquid in a high-pressure stainless-steel cylinder. The gas thus separated from the liquid was depressurized by means of a back-pressure regulator and was vented to atmosphere after passing through a flowmeter. The water from the separator was drained continuously.

The system was heated to the required temperature with low-pressure gas flowing at a low flow rate. After attaining the operating temperature, the pressure was increased by starting the compressor. The water pump was started simultaneously. The operating pressure was attained by adjusting the pressure regulator and the back-pressure regulator; the pressure drop between these points controlled the gas flow rate. The water was pumped at the required flow rate by adjusting the pump to the predetermined value, which was verified by measuring the amount of water collected for a known time in the sample tank. The system was maintained at the operating conditions for one hour before taking samples. The sample was collected in the sample collector by diverting flow using a valving system. After the desired time, flow was restored to the liquid waste tank, and the sample was drained from the collection tank. This procedure was followed since it did not result in a loss of system pressure when the liquid sample was drained.

Product quantification was accomplished using UV/Vis Diode Array and Atomic Absorption spectrophotometry. The UV/Vis Diode Array spectrophotometer (HP 8452A) was calibrated for chromium using prepared standard samples in the concentration range 0.05 ppm to 30.0 ppm chromium in water. Quantitative analysis was accomplished using a total response of $350 < \lambda < 370$ nm, the width of the λ_{max} peak identified from the calibration experiments. The effluent samples were analyzed for Cr ion concentration off-line using the UV spectrophotometer immediately after collection. An atomic absorption spectrophotometer (Perkin Elmer 2380) was also calibrated with prepared standards for analysis of nickel and chromium in the effluent. The chromium analysis was consistent with the results from the UV/Vis procedure. The detection limit on this instrument was found to be 0.02 ppm for chromium and 0.05 ppm for nickel.

Gas analysis was performed with an HP 5890 gas chromatograph (GC) and a thermal conductivity detector (TCD). A 15-ft × 1/8-in. 60/80 Carboxen packed column was used. The GC was operated at 50°C for 3 min, the temperature was increased to 150°C at a rate of 15°C/min. The final temperature of 150°C was retained for 3 min.

There was minimal deposition of chromium in the heat exchanger. After several runs, the heat exchanger was disconnected from the system and was washed with 20% sulfuric acid and 20% nitric acid. The effluent was analyzed for chromium ion. The analysis indicated the concentration of chromium ion as 0.15 ppm. Visual observation after removing the heat exchanger indicated no chromium precipitation. This level of deposition was negligible compared to the level of chromium observed in the effluent stream.

Feed conditions were defined in terms of molar flow rates. Since the reactant feed consists of water, oxygen, and nitrogen, and the water content varied from 60 to 90 mol %, the Peng–Robinson equation of state with the van der Waals mixing rules (Sandler, 1989) was used to calculate the fluid density. Conversion to volumetric flow rates and then superficial velocity could be made. Residence time was calculated by dividing the reactor volume by the volumetric flow rate. The concentration of the reactants (mol/L) at the reaction conditions were estimated by dividing the molar flow rate by volumetric flow rate.

The process variables were changed randomly to avoid any systematic error. All the experiments were conducted at a constant pressure of 238 atm and residence time of approximately 6 s. The reactivity of chromium oxide with supercritical water was studied between $390°C < T < 420°C$ and oxygen and water concentrations between 0.005 mol/L $< [O_2] < 0.36$ mol/L (corresponding to $7.8 \times 10^{-4} < [O_2] < 0.078$ mole fraction) and 2.88 mol/L $< [H_2O] < 6.38$ mol/L, respectively. Experiments were conducted at a given set of operating conditions until a steady-state value for the concentration of chromium ion in the effluent was obtained. In case of any process disturbances, the conditions were maintained until the steady-state value was obtained again.

Results

The effect of the feed concentration of oxygen on the effluent concentration of chromium ion at 400°C and 238 atm is shown in Figure 2 as a function of run time. The effect of oxygen concentration was tested by changing the feed gas in

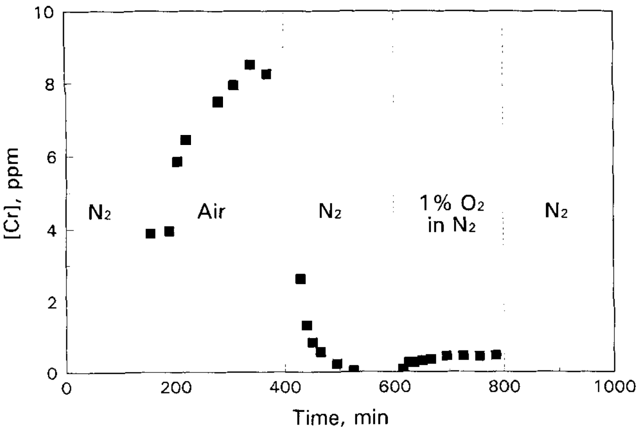

Figure 2. Transient response of chromium effluent concentration following changes in reactor inlet oxygen concentration at 400°C and 238 atm.

the following manner: nitrogen, air, nitrogen, 1% oxygen in nitrogen, and finally nitrogen. The effluent chromium concentration changed to reflect the change in the oxygen concentration of the feed, but with a significant time delay, on the order of 200 min. The effluent oxygen concentration did not vary significantly from the feed concentration. When oxygen was not present in the feed, the concentration of chromium in the effluent dropped below the detectability limit of the UV, approximately 0.05 ppm; no data are shown in Figure 2 for these points. These results qualitatively reveal that increasing oxygen concentration led to enhanced extraction of chromium ion.

Ion exchange was used to determine the oxidation state of the Cr extracted in the effluent. The effluent was tested using both cationic (Amberlite IRC-718, Amberlite DP-1) and anionic resins (Amberlite IRA-400). Identification was based on the principle that Cr(III) would be adsorbed on the cationic resin but not the anionic resin, whereas Cr(VI) would be adsorbed on the anionic resin only. Standard solutions prepared from K_2CrO_4 and $CrCl_3 \cdot H_2O$ revealed that this indeed was the case, and that the amount of adsorption could be quantified. Analysis of the effluent from the resins with both UV and AA spectroscopy revealed that no adsorption was obtained for the cationic resin, but that the effluent samples were completely depleted of chromium using the anionic resin. Thus it was concluded that the Cr extracted from the reactor was recovered as Cr(VI), probably as chromic acid, H_2CrO_4. This is consistent with theoretical result, reported in the form of a Pourbaix diagram for the Cr–H_2O system at elevated temperature and pressure (Huang et al., 1989), which indicates that there are no stable chromium oxide species within the region of neutral water. Depending on the pH of the solution, chromium will be present as either H_2CrO_4, $HCrO_4^-$, $Cr_2O_7^{2-}$, or CrO_4^{2-}, with increasing alkalinity. Thus, an equilibrium reaction is predicted by these theoretical calculations.

Because of concerns about reactor corrosion, the effluent samples were tested regularly for the presence of nickel ions. At all operating conditions, the concentration of Ni ion was found to be less than 2 ppm, the value obtained at the highest oxygen concentration. This suggests that some corrosion of the reactor walls did occur during these experiments. However, Hastelloy C-276 contains more Ni than Cr (composition of Hastelloy C-276 is Ni: 45.02–63.48%, Cr: 14.5–16.5%, Mo: 15–17%, Fe: 4–7%, W: 3–4.5%, and C: 0.02%). Since the nickel content in the effluent was generally more than an order of magnitude less than the chromium content and nickel represents a larger portion of the reactor material, it can be presumed that any contribution of corrosion to the Cr effluent results would be small compared to extraction from the catalyst bed.

Table 1. Experimental Data

Run No.	Temp. °C	Water Conc. mol/L	Oxygen Conc. mol fr.	Residence Time s	Chromium Effluent Conc. μmol/L
23	390	3.43	0.069	5.23	18.3
25	390	4.39	0.045	5.24	22.0
21	390	5.63	0.013	5.37	18.4
14	390	5.66	0.025	5.40	26.5
16	390	5.66	0.025	5.40	27.3
13	390	6.35	0.0008	5.58	5.43
10	390	6.36	0.009	5.60	21.1
24	390	6.38	0.017	5.64	25.3
29	400	3.16	0.074	5.88	16.0
17	400	3.88	0.0025	5.70	3.92
7	400	3.88	0.054	5.81	20.7
18	400	5.09	0.0014	5.99	4.86
20	400	5.05	0.016	6.00	19.3
8	400	5.06	0.030	6.04	24.8
4	400	5.70	0.0009	2.50	3.65
2	400	5.76	0.0009	3.14	3.85
5	400	5.69	0.0009	4.44	4.78
1	400	5.70	0.0009	6.19	5.15
3	400	5.71	0.0009	8.83	5.56
9	400	5.72	0.010	6.21	21.4
6	400	6.20	0.014	6.43	28.2
28	420	2.88	0.078	6.29	14.0
19	420	3.66	0.0026	6.35	3.16
26	420	3.73	0.052	6.44	22.1
15	420	4.39	0.036	6.56	29.6
12	420	4.97	0.0012	6.70	4.80
22	420	5.14	0.019	7.67	20.4
27	420	5.04	0.023	6.80	31.8
11	420	5.67	0.013	7.65	23.2

Twenty-nine independent reaction experiments were completed at three reaction temperatures and over a wide range of oxygen and water concentrations and residence times. The results from these runs are reported in Table 1. Included within this data are replicate runs (14 and 16) that reveal the quality of the experimental program. More detailed analysis of all of the data reveals that the entire data set is internally consistent according to the following description.

The effect of oxygen concentration (estimated from the feed composition based on the density of the fluid within the reactor) on the concentration of chromium ion in the effluent was determined at 390°C (runs 10, 13 and 24), 400°C (runs 8, 18 and 20), and at 420°C (runs 19 and 26 or runs 12 and 27). In each case, increasing the oxygen concentration at otherwise identical reaction conditions led to an increase in the concentration of chromium in the effluent. At low oxygen concentrations, relatively low concentration of chromium is detected in the effluent and increasing oxygen leads to a dramatic increase in the chromium concentration in the effluent.

At high oxygen concentration, the effect of increasing oxygen is less pronounced, suggesting that there could be a saturation point above which the concentration of chromium in the effluent becomes independent of the oxygen concentration within the reactor.

The effect of water concentration on the concentration of chromium ion in the effluent is revealed at 390°C by runs 14, 23 and 25; at 400°C by runs 1, 17 and 18; and at 420°C by runs 15, 26, 27 and 28. In each sequence of experiments, an increase in the concentration of water was accompanied by an increase in the concentration of chromium in the effluent, despite the fact that the oxygen concentration decreased simultaneously. It was indicated in the preceding paragraph that a decrease in the oxygen concentration should lead to a decrease in the concentration of chromium in the effluent. Thus, if the water concentration were increased at constant oxygen mole fraction, a significant increase of the chromium ion concentration in the effluent would be expected.

After completion of one set of experiments, the catalyst was removed from the reactor. Visual observation revealed that the top portion of the bed was pink in color, the bottom was green, and the intermediate section contained both green and pink particles. The original color of the catalyst was green, whereas a catalyst mostly depleted of chromium would be expected to become pink and eventually white if all of the chromium is removed (Mellor, 1931). The used catalyst was subjected to X-ray diffraction (XRD) analysis, using an Omni Instruments unit with a detection limit of 1% chromium by weight. The XRD results indicated that the top portion of the bed was depleted of chromium oxide below the detection limit of the instrument. The only compound identified in this region was the catalyst support, aluminum oxide. This observation suggests that depletion of chromium from the support moved along the length of the reactor, from the entrance of the bed to the exit, with increasing time on-stream.

This breakthrough phenomenon could be explained through a chemical reaction in which one of the reactants is completely depleted at some point along the length of the bed. However, the effluent gas analysis indicated that there was no measurable decrease in oxygen concentration through the reactor, and thus oxygen could not be a rate-limiting reactant.

An alternative explanation is that a reversible chemical reaction occurs that converts solid chromium oxide into soluble chromium. Experiments were conducted to determine whether chromium could be deposited on the solid, thereby confirming the reversible nature of the reaction. The experiments were performed by feeding prepared chromate solutions of various concentrations to the reactor. This experiment was conducted at 400°C and 238 atm at two different oxygen and water concentrations; the chromium effluent concentration is reported in Figure 3. The concentration of chromate in the effluent remained essentially unchanged, independent of Cr concentration in the feed. This result indicates that deposition is taking place, according to the following analysis. If no deposition was occurring, the concentration of Cr in the effluent should have increased as the concentration of Cr in the feed increased. But the results indicate that the effluent concentration was not effected by the feed concentration. Second, when the alumina packing and the catalyst were removed from the reactor after completion of these experiments, a layer of precipitated chromium was observed on the top portion of the alumina packing. The deposition likely occurred when the feed concentration was greater than the effluent concentration, indicating that the chromate precipitated before reaching the catalyst layer.

In any reaction process involving fluid–solid reactions, the rate of mass transfer may be a limiting process. This could be true regardless of any equilibrium reaction that might occur within the reactor. The effect of mass transfer was not explicitly measured, but can be obtained by considering the effect of fluid volumetric flow rate on the rate of chromium extraction, which is reported in Figure 4. In this figure, the rate of extraction is derived from the concentration of chromium measured in the effluent and the volumetric flow rate of the fluid in the reactor. The results are reported in terms of square root of the Reynolds number ($N_{Re} = \rho u d_p/\mu$), as previous data in packed-bed reactors have indicated that this is the expected effect of flow rate in a mass-transfer process

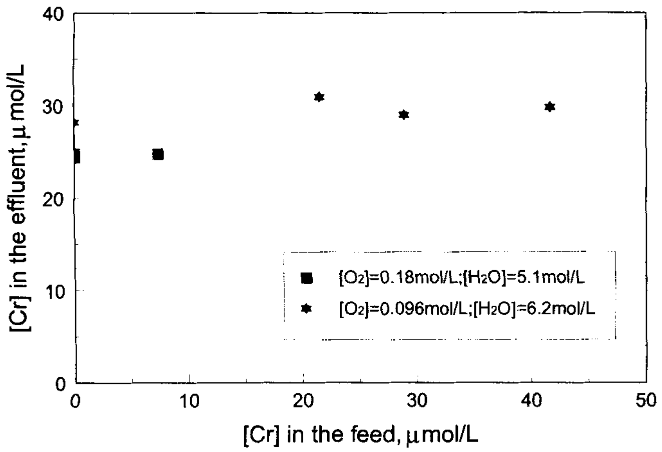

Figure 3. Influence of chromate concentration in the feed on the chromium effluent concentration at 400°C and 238 atm.

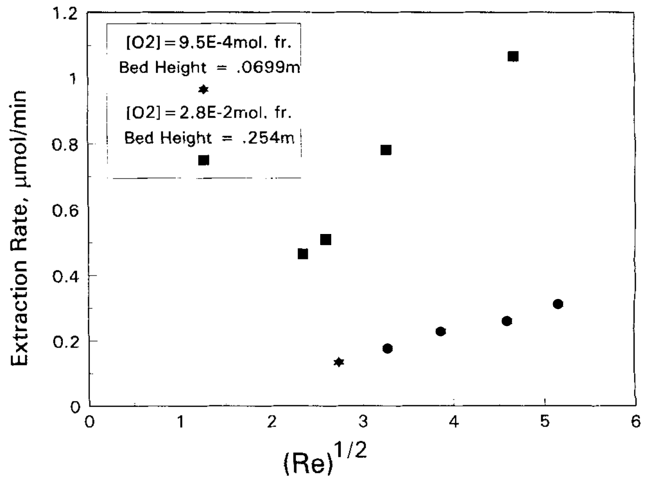

Figure 4. Evaluation of possible external mass-transfer effects through correlation of the rate of chromium extraction with the Reynolds number.

Table 2. Effect of Organic Compounds on the Cr Concentration in Effluent*

Temp. °C	Organic Species	$[O_2]$ mol/L	$[H_2O]$ mol/L	Conv. %	CO_2 Yield %	[Cr] μmol/L
390	None	0.16	5.7	—	—	26.5
390	Phenol	0.16	4.9	98.6	36.6	16.7
400	None	0.28	3.9	—	—	20.7
400	Benzene	0.27	3.9	19.03	2.88	0.22

*source: Ding, 1995.

(Carberry, 1976). Note that as the volumetric flow rate changed, so did the residence time. This is contrary to the normal fashion in which these data are obtained. However, these data are clearly linear in $N_{Re}^{1/2}$, indicating that mass transfer may have a role in the rate of chromium extraction.

If external mass transfer is rate-limiting, then this should determine the dependence of the extraction rate on the concentration of oxygen. In the case where transport of oxygen from the bulk to the catalyst surface is rate-limiting, one would expect that the rate of extraction is first order in oxygen. In this case, doubling the oxygen concentration would double the extraction rate. Comparison of the results from runs 21 and 14 reveal that this was not observed experimentally. These experiments were performed at the same residence time (and thus equivalent volumetric flow rates), and yet when the oxygen concentration was doubled, the extraction of chromium increased by less than 50%. Similar results are revealed in experiments 20 and 8. If transport of chromate from the catalyst surface to the bulk fluid is rate-limiting, then there should be no dependence of extraction rate on oxygen concentration. This is clearly contrary to the experimental data. Thus, despite the dependence of extraction rate on Reynolds number, it is unlikely that mass transfer is rate-limiting.

Because of the interest in using a heterogeneous catalyst during SCWO, the effect of two different organic compounds, benzene and phenol, on the Cr effluent concentration was studied. The results in Table 2 indicate that the introduction of either organic reactant led to a decrease in the Cr effluent concentration. Since it was previously determined that oxygen concentration is an important variable in determining the extraction of Cr ion from the catalyst, the addition of an organic reactant may impact the extraction of chromium from the catalyst in two ways. First, because an oxidation reaction is occurring, the concentration of oxygen in the fluid phase will be decreased. Thus, the actual oxygen concentration will be less than that fed to the reactor. Second, if a heterogeneous oxidation reaction is actually occurring, the organic species is likely adsorbed onto the active sites of the catalyst. Since the oxygen adsorption is believed to be important in the extraction of Cr ions from the catalyst, competitive adsorption of the organic species would decrease the oxygen concentration actually adsorbed on the catalyst, thereby decreasing the extraction rate of Cr from the catalyst.

Discussion

A theoretical model has been developed that describes the extraction process in terms of reaction and dissolution of Cr from the catalyst surface to the fluid phase. A rate expression, consistent with the experimental observations and literature reports, is developed to describe the fluid–solid reaction. The continuity equation is then used to describe flow in the fluid phase. Finally, the model is used in conjunction with the experimental data to evaluate best-fit parameters. In the development of this model, any limitation imposed by the rate of mass transfer has been neglected, since the data do not clearly support a mass-transfer limitation. Thus, the rate constants calculated from this model should be considered as effective rate constants rather than intrinsic values. The validity of neglecting mass-transfer limitations will then be justified based on theoretical calculations of the mass-transfer coefficient.

In previous work, the dissolution of chromium oxide in oxygenated alkaline media has been described through reaction with oxygen and hydroxyl ions (Blesa and Maroto, 1986)

$$Cr_2O_3 + 3/2\ O_2 + 4\ OH^- \rightarrow 2\ CrO_4^{2-} + 2H_2O. \tag{1}$$

Under the reaction conditions used in our experiments, the pH of water can be estimated to be substantially greater than 7 (Franck, 1970), suggesting that the chemistry indicated in Eq. 1 may be occurring. However, because of the water concentration and its low dissociation constant ($K_w < 10^{-20}$) under supercritical conditions, the reaction is more likely to involve oxidative hydration, giving chromic acid directly as a product

$$Cr_2O_3 + 3/2\ O_2 + 2\ H_2O \rightleftharpoons 2H_2CrO_4. \tag{2}$$

The overall chemical reaction written as Eq. 2 may be described through a reaction cycle, developed from the work of Zecchina et al. (1971). The reaction is initiated by dissociative chemisorption of oxygen onto chromium oxide,

$$1/2\ O_2 + Cr_2O_3 \xrightleftharpoons{2xH_2O} 2[CrO_2 \cdot xH_2O]. \tag{3}$$

Disproportionation of hydrated chromia surface complex gives

$$2[CrO_2 \cdot xH_2O] \rightleftharpoons H_2CrO_4 + [CrO \cdot (x-1)H_2O]. \tag{4}$$

The surface complex thus formed, $[CrO \cdot (x-1)\ H_2O]$, is again saturated with water and is an active site for dissociative chemisorption of oxygen,

$$[CrO \cdot (x-1)H_2O] + H_2O + 1/2\ O_2 \rightleftharpoons [CrO_2 \cdot xH_2O]. \tag{5}$$

Using this reaction description, and assuming that the dissociative chemisorption of oxygen in the presence of water (Eq. 5) is rate-limiting, provides a rate expression of the Langmuir–Hinshelwood form

$$-r_{[Cr_2O_3]} = \frac{k_f\sqrt{K[O_2]}\,[H_2O]^{1.75}q - k_r[Cr]}{\left[1+\sqrt{K[O_2]}\right]}, \tag{6}$$

where q is defined as the moles of reactant present per unit total reactor volume. The exponent on the water concentration represents the average number of water molecules adsorbed on an active site. Although arbitrarily chosen to be 1.75, this value can be justified from previous experimental results reported for supercritical water oxidation, wherein the dependence of reaction rate on water concentration has been found to be between 1.5 and 2 (Savage et al., 1995).

The reversibility described in Eq. 2 is derived from our experimental results, but justified based on literature reports. When 2N H_2CrO_4 was exposed to hydrogen, a heavy grayish-violet, slightly crystalline precipitate of chromic oxyhydroxide, $Cr_2O_3 \cdot H_2O$, was formed (Mellor, 1931). When air was used in place of hydrogen, smaller crystals of Cr_2O_3 were formed, with a portion being converted to chromic acid. Hoar and Evans (1932) showed that in the presence of base and water, precipitation of chromates to hydrated chromic oxide may occur.

The analysis of chromium concentration in the fluid phase begins with the continuity equation, which can be written, assuming plug flow, as

$$u\frac{\partial[\mathrm{Cr}]}{\partial z}+\frac{\partial[\mathrm{Cr}]}{\partial t}=r_{[\mathrm{Cr}]}, \tag{7}$$

where here and in the ensuing discussion, all the concentrations are based on the total reactor volume. If we assume that a pseudo steady state has been achieved within the reactor, then the chromium concentration in the effluent can be approximated as being invariant in time, and Eq. 7 can be approximated as

$$u\frac{\partial[\mathrm{Cr}]}{\partial z}=r_{[\mathrm{Cr}]}. \tag{8}$$

Now, by making use of the inlet boundary condition, $[\mathrm{Cr}]=0$ at $z=0$, Eq. 8 can be solved analytically, depending upon the specific reaction kinetics chosen to represent the rate of reaction. Although there is no time dependence explicitly included in Eq. 8, this dependence can remain through the dependence of the solid concentration on time, which may be included in the reaction kinetics.

Next, we note that a chromium balance on the solid phase can be simply written as

$$\frac{\partial q}{\partial t}=-r_{[\mathrm{Cr_2O_3}]} \tag{9}$$

with an initial condition that $q=q_O$ at $t=0$. Since the change in oxygen and water concentrations along the length of the bed are small, and Cr concentration in the fluid phase is independent of time after reaching pseudo steady state, Eq. 9 can be solved directly after substitution of the rate expression (Eq. 6) to provide

$$q=q_o\exp(-Pt)+\frac{k_r[\mathrm{Cr}]}{k_f\sqrt{K[\mathrm{O_2}]}\,[\mathrm{H_2O}]^{1.75}}\{1-\exp(-\mathrm{Pt})\}, \tag{10}$$

where

$$P=\frac{k_f\sqrt{K[\mathrm{O_2}]}\,[\mathrm{H_2O}]^{1.75}}{1+\sqrt{K[\mathrm{O_2}]}}$$

From the reaction stoichiometry given in Eq. 2, it follows that

$$r_{[\mathrm{Cr}]}=-2r_{(\mathrm{Cr_2O_3}]}. \tag{11}$$

Solution for the chromium effluent concentration can be obtained by solving Eq. 8 at the given boundary conditions, with Eq. 10 providing the necessary relationship between q and [Cr]. Solution is obtained as

$$[\mathrm{Cr}]=\frac{k_f\sqrt{K[\mathrm{O_2}]}\,[\mathrm{H_2O}]^{1.75}q_o}{k_r}\{1-\exp(-Xz)\}, \tag{12}$$

where

$$X=\frac{2k_r\exp(Pt)}{u\left(1+\sqrt{K[\mathrm{O_2}]}\right)}$$

The chromium oxide concentration in the reactor can now be obtained as a function of time and position by eliminating [Cr] between Eq. 10 and Eq. 12. This solution is obtained as

$$\frac{q}{q_o}=1-\exp(-Xz)\{1-\exp(-Pt)\}. \tag{13}$$

Using the experimental results and the analytical solution described by Eq. 12, it is possible to estimate the values of the constants. A simplex multivariable search routine was used, as described in Press (1986), which minimized the sum of squares error between the predicted effluent concentration and the experimental values

$$\min\sum_{N=1}^{\mathrm{NDATA}}\{[\mathrm{Cr}]_{\mathrm{Pred}}-[\mathrm{Cr}]_{\mathrm{exp}}\}^2, \tag{14}$$

where NDATA is the number of experimental measurements. The values of the constants, which correspond to two rate constants and one adsorption coefficient, are functions of temperature. Thus, the evaluation of the three fit parameters was performed independently using the data at each reaction temperature.

Figure 5 compares the model prediction, containing the best fit values of the parameters (Table 3), with the experimental measurements. Over the entire range of experiments, a fairly good agreement has been obtained between the predicted and the experimental values. The data correlated by this model represent a wide range of inlet compositions and reaction temperatures.

The mass transfer of chromate ion from the solid surface to the bulk fluid was considered as a possible rate-limiting step in the development of the model. The mass-transfer coefficient for chromate ion was calculated from the correlation

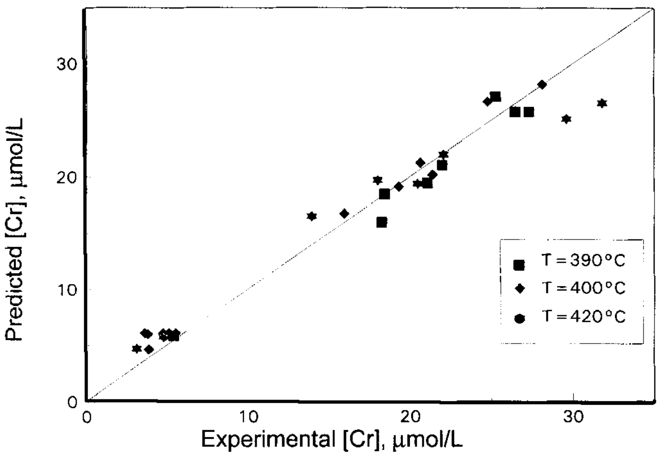

Figure 5. Parity plot: model prediction vs. experimental values of chromium effluent concentration.

as given by Chen et al. (1993). The diffusion coefficient for chromate ion was calculated from the Stokes–Einstein equation, while the viscosity of the bulk fluid at the elevated conditions was calculated from the correlations given by Paulaitis et al. (1986). The estimated mass-transfer coefficient was always at least an order of magnitude greater than the value of the reverse rate constant reported in Table 3, indicating that the rate of mass transfer was fast compared to the rate of reaction.

Although the data at each temperature were fit independent of the reaction model, the evaluated rate constants must conform to expected chemical criteria so that the model is satisfactory. The first of these criteria is that the rate constants should be consistent with the Arrhenius equation,

$$k = Ae^{(-E_A/RT)}. \tag{15}$$

The best-fit values of the two rate constants are plotted in Arrhenius fashion in Figure 6a, and the values for the activation energy given in Table 3. The estimated value of E_A = 169.5 kJ/mol for the reaction between oxygen and Cr_2O_3 in supercritical water may be compared with previous values obtained for this reaction in acidic media. Several values have been reported previously and are indicated in Table 4. The activation energy obtained in the current work is 4 to 5 times greater than those values obtained for acid catalyzed reaction. This is not unreasonable, considering that the presence of dissociated ions should catalyze the initiation reaction according to Eq. 1, and dissociation is unlikely in supercritical water.

Table 3. Best-fit Values of the Model Parameters (Eq. 12) and Correlation of Parameters with Respect to Temperature Based on Eq. 15

Temp. °C	k_f $(\mathrm{mol/cm^3})^{-1.75}\cdot\mathrm{s}^{-1}$	k_r s^{-1}	K $(\mathrm{mol/cm^3})^{-1}$
390	2.02	0.797	13.85
400	3.36	1.03	10.52
420	7.32	1.42	5.55
Activation energy, kJ/mol	169.5	71.7	$\Delta H_{ads} = 117.5$
A	$4.4E+13$	$3.63E+05$	$7.82E-09$

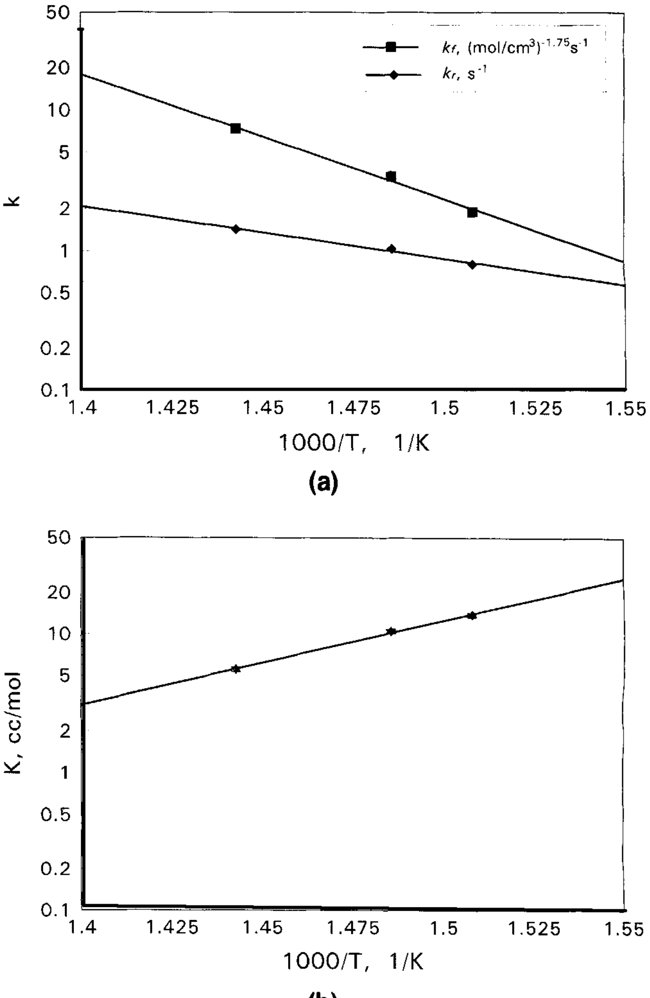

Figure 6. (a) Estimation of the Arrehenius parameters for the best-fit values of the rate constants; (b) estimation of heat of adsorption parameters using the van't Hoff plot.

A further test of the consistency of the model is through a van't Hoff relationship, which describes the temperature dependence of the adsorption coefficient, K, and leads to a calculation of the heat of adsorption for oxygen onto Cr_2O_3. The van't Hoff plot is indicated in Figure 6b, and reveals a heat of adsorption as 117.5 kJ/mol. Previously, Trapnell

Table 4. Comparison of Estimated Activation Energy at 238 atm in Supercritical Water with Values Reported for the Oxidation of Cr_2O_3 at Ambient Conditions

	Activation kJ/mol
Experimental Value	169.5
In 8-M H_2SO_4 + 40% acetone*	35.2
H_2SO_4*	31.0,32.7,47.8
HF*	41.9,42.6

*Gorichev and Kipriyanov, 1981.

(1955) reported a value of 154.8 kJ/mol for the initial adsorption of oxygen on Cr_2O_3 at room temperature. The value obtained in the current work was estimated for 400°C and for a surface that should be saturated with water. The difference is not unreasonable, considering the large variation in both temperature and water concentration between the previous and the current work.

The best fit parameters can be subjected to further chemical kinetic criteria, as described by Carberry (1976)

$$\Delta S < 0$$

$$|\Delta S| < S_{\text{gas}}$$

$$|-\Delta S| > 10 \text{ entropy units}$$

$$|-\Delta S| < 12.2 - 0.0014\, \Delta H_{\text{ads}},$$

where ΔS is the entropy change of reaction, which can be estimated from the intercept in the van't Hoff plot. The current data provide $\Delta S = -0.155\ \text{kJ}\cdot\text{mol}^{-1}\cdot\text{K}^{-1}$. This value satisfies all of the above criteria, providing further evidence that the model parameters have chemical significance.

Using the model, it is now possible to describe the chromium concentration profile in the solid phase as a function of time and position within the reactor. This result is shown in Figure 7, where the solid lines represent time on stream below 214 h. the total duration of all experiments considered within this article, while the dashed lines represent extrapolation to longer on-stream times. These concentration profiles were obtained using the constants of Table 3 and the model result given by Eq. 13. However, the experimental data were obtained in a piecewise continuous fashion. As a result, simply substituting the on-stream time into Eq. 13 did not yield an accurate approximation of the experimental situation. Rather, solution could be obtained by reinitializing q_O for each experimental condition and resetting $t_2' = t_2 - t_1$, for example, The model result reveals the movement of an extraction front down the length of the bed. For an accumulated time on stream of 214 h, the actual time on stream within these experiments, the model predicts greater than 80% removal of chromium from the first 0.5 cm of the bed, with virtually no loss of catalyst from the bottom two-thirds of the bed. This prediction matches qualitatively well with the visual observation of the bed following the experiment.

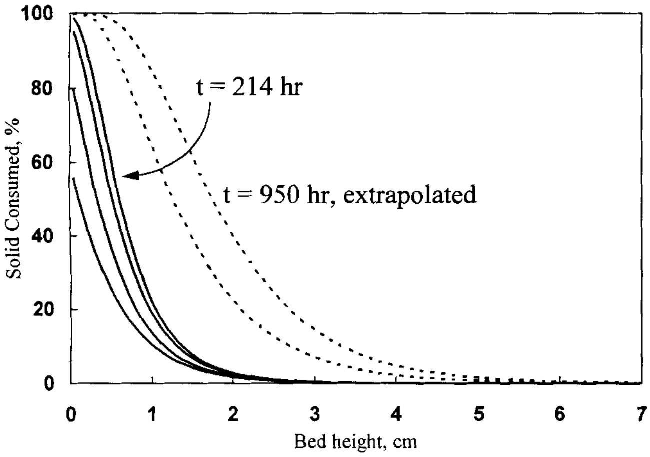

Figure 7. Model prediction and extrapolation of chromium oxide consumption as a function of bed depth and time on stream.

Conclusion

The reaction of Cr_2O_3 with oxygen in supercritical water has been investigated as a means of studying the stability of a catalyst during supercritical water oxidation. The chromium is slowly depleted from the bed. The rate of depletion is a function of reaction temperature, oxygen and water concentration, and fluid flow rate. Because chromium could be deposited onto the bed, it was determined that the reaction must occur reversibly.

The depletion of Cr_2O_3 was modeled using a plug flow reactor model. Reaction was assumed to occur by dissociative adsorption of oxygen on a hydrated chromium oxide surface. The Cr effluent concentration was used to determine best-fit values for the constants within a Langmuir–Hinshelwood-type rate expression; the activation energy and heat of adsorption were not inconsistent with previously reported values for the reaction in acid solution. The model was able to predict not only the effluent concentration, but also qualitatively the concentration of Cr remaining on the solid catalyst.

These results have substantial implication in the potential use of a heterogeneous catalyst during supercritical water oxidation, in that they reveal the limitation of reaction of the solid catalyst with components in the fluid phase. These results may also be applied to the issue of corrosion during supercritical water oxidation, since Cr metal is frequently used as a component in the metal alloy for the materials of construction of the reactor. The formation of a passivated Cr_2O_3 has been described as the stable metal surface in such a case. When used for SCWO, however, it is clear that the Cr_2O_3 is reactive, minimizing the corrosion resistance of the metal alloys.

Acknowledgments

This work has been funded under a grant from the National Science Foundation, number CTS 8909940. Support for Z.-Y. D. was provided by NASA through the Jove program, Grant NAG8-005. Additional support has been received from the University of Tulsa Office of Research. The authors would also like to acknowledge Dr. Tom Harris, Department of Chemistry, The University of Tulsa, for his assistance with the use of the Atomic Absorption Spectrometer.

Notation

$[Cr]$ = concentration of chromium in the effluent, mol/cm^3
d_p = particle diameter, cm
$[H_2O]$ = concentration of water, $\text{mol}\cdot\text{cm}^{-3}$
k_f = forward rate constant, $(\text{mol/cm}^3)^{-1.75}\cdot\text{s}^{-1}$
k_r = reverse rate constant, s^{-1}
$[O_2]$ = concentration of oxygen, $\text{mol}\cdot\text{cm}^{-3}$
q_O = initial concentration of chromium oxide in the reactor, $\text{mol}\cdot\text{cm}^{-3}$
$r_{[Cr]}$ = rate of generation of chromic acid, $\text{mol}\cdot\text{cm}^{-3}\cdot\text{s}^{-1}$
t = real time, s
u = superficial velocity, $\text{cm}\cdot\text{s}^{-1}$
z = distance along the reactor length, cm

Greek letters

μ = fluid viscosity, at reaction conditions, $\text{g}\cdot\text{cm}^{-1}\cdot\text{s}^{-1}$
ρ = fluid density at reaction conditions, g cm^{-3}

Literature Cited

Barner, H. E., C. Y. Huang, T. Johnson, G. Jacobs, and M. A. Martch, "Supercritical Water Oxidation: An Emerging Technology," *J. Hazardous Mat.*, **31**, 1 (1992).

Blesa, M. A., and A. J. G. Maroto, "Dissolution of Metal Oxides," *J. Chim. Phys.*, **83**, 697 (1986).

Bramlette, T. T., B. E. Mills, K. R. Hencken, M. E. Brynildson, S. C. Johnston, J. M. Hruby, H. C. Feemster, B. C. Odegard, and M. Modell, "Destruction of DOE/DP Surrogate Wastes with Supercritical Water Oxidation Technology," *SAND90-8229*, Sandia Rep., Sandia Labs, November (1980).

Carberry, J. J., *Chemical and Catalytic Reaction Engineering*, McGraw-Hill, New York, p. 413 (1976).

Chen, J. C., Y. T. Shah, and M. A. Abraham, "Liquid Phase Transport Properties in a High Pressure Packed Column," *Chem. Eng. Commun.*, **125**, 1 (1993).

Copson, H. R., and W. E. Berry, "Quantification of Inconel for Nuclear Power Plant Applications," *Corrosion-NACE*, **16**, 123 (1960).

Dell'Orco, P. C., E. F. Gloyna, and S. Buelow, "Oxidation Processes in the Separation of Solids from Supercritical Water," *Supercritical Fluid Engineering Science: Fundamentals and Applications*, E. Kiran, and J. F. Brennecke, eds., ACS Symposium Series 514, American Chemical Society, Washington, DC (1992).

Ding, Z. Y., N. V. K. S. Aki, and M. A. Abraham, "Catalytic Supercritical Water Oxidation: An Approach for Complete Destruction of Aromatic Compounds," presented as a part of the Symp. on Supercritical Fluids, AIChE Meeting, San Francisco (1994).

Ding, Z. Y., "Catalytic Supercritical Water Oxidation of Aromatics: Benzene, Phenol, and 1,3-Dichlorobenzene on Metal Oxides," PhD Diss., The Univ. of Tulsa, Tulsa, OK (1995).

Franck, E. U., "Water and Aqueous Solutions at High Pressure and Temperatures," *Pure Appl. Chem.*, **24**, 13 (1970).

Frisch, M. A., "Supercritical Water Oxidation of Acetic Acid Catalyzed by CeO_2/MnO_2," MS Thesis, Univ. of Texas-Austin, Austin (1992).

Gorichev, I. G., and N. A. Kipriyanov, "Kinetics of the Dissolution of Oxide Phases in Acids," *Russ. J. Phys. Chem.*, **55**(11), 1558 (1981).

Hearn, B., M. R. Hunt, and A. Hayward, "Solubility of Cupric Oxide in Pure Subcritical and Supercritical Water," *J. Chem. Eng. Data*, **14**(4), 442 (1969).

Helling, R. K., and J. W. Tester, "Oxidation Kinetics of Simple Compounds in Supercritical Water: Carbon Monoxide, Ammonia and Ethanol," ScD Diss., MIT, Cambridge, MA (1986).

Hoar, T. P., and U. R. Evans, "The Passivity of Metals: VII. The Specific Function of Chromates," *Amer. Chem. Soc. J.*, 2476 (1932).

Holser, W. T., and C. J. Schneer, "Hydrothermal Magnetite," *Geol. Sci.*, **72**, 369 (1961).

Huang, S., K. Daheling, T. E. Carleson, P. Taylor, C. Wai, and A. Propp, "Thermodynamic Analysis of Corrosion of Iron Alloys in Supercritical Water," *Supercritical Fluid Science and Technology*, K. P. Johnston, and M. L. Penninger, eds., ACS Symp. Ser. 406, American Chemical Society, Washington, DC, (1989).

I-Ming, C., and H. P. Eugster, "Solubility of Magnetite in Supercritical Chloride Solutions," *Amer. J. Sci.*, **277**, 1296 (1977).

Japas, M. L., and E. U. Franck, "High Pressure Phase Equilibria and PVT-Data of the Water-Nitrogen System to 673 K and 250 MPa," *Ber. Buns. Phys. Chem.*, **89**(7), 793 (1985).

Jin, L., Z. Ding, and M. A. Abraham, "Catalytic Supercritical Water Oxidation of 1,4-Dichlorobenzene," *Chem. Eng. Sci.*, **47**(9–11), 2659 (1992).

Marshall, W. L., and E. U. Franck, "Ion Product of Water Substance, 0-1000°C, 1-10,000 Bars, New International Formula and its Background," *J. Phys. Chem. Ref. Data*, **10**(21), 295 (1981).

Martynova, O. I., "Some Problems of the Solubility of Involatile Inorganic Compounds in Water Vapor at High Temperatures and Pressures," *Russ. J. Phys. Chem.*, **38** (5), 587 (1964).

McIntyre, N. S., D. G. Zetaruk, and D. Owen, "XPS Study of the Initial Growth of Oxide Films on Inconel 600 Alloy," *Appl. Surf. Sci.*, **2**, 55 (1978).

McIntyre, N. S., D. G. Zetaruk, and D. Owen, "X-Ray Photoelectron Studies of the Aqueous Oxidation of Inconel-600 Alloy," *J. Electrochem. Soc.: Electrochem. Sci. Technol.*, **126**(5), 750 (1979).

Mellor, J. W., *A Comprehensive Treatise on Inorganic and Theoretical Chemistry*, Vol. XI, Longmans, Green, New York (1931).

Morey, G. W., and J. M. Hesselgesser, "The Solubility of Some Minerals in Superheated Steam at High Pressures," *Econ. Geol.*, **46**, 821 (1951).

Otsuka, N., and H. Fujikawa, "Scaling of Austenitic Stainless Steels and Nickel-Base Alloys in High Temperature Steam at 973 K," *Corrosion*, **47**(4), 240 (1991).

Paulaitis, M. E., V. J. Krukonis, R. T. Kurnik, and R. C. Reid, "Supercritical Fluid Extraction," *Rev. Chem. Eng.*, **1**(2), 179 (1986).

Postlethwaite, J., R. J. Schoular, and M. H. Dobbin, "Localized Corrosion of Molybdenum-Bearing Nickel Alloys in Chloride Solutions," *Corrosion-NACE*, **44**(4), 199 (1988).

Press, W. H., B. P. Flannery, S. A. Teukolsky, and W. T. Vetterling, *Numerical Recipes. The Art of Scientific Computing*, Cambridge Univ. Press, Cambridge, England (1986).

Quist, A. S., "The Ionization Constant of Water of 800°C and 4000 Bars," *J. Phys. Chem.*, **74**(18), 3396 (1970).

Robertson, J., "The Mechanism of High Temperature Aqueous Corrosion of Steel," *Corr. Sci.*, **29**(11/12) 1275 (1989).

Sandler, S. I., *Chemical and Engineering Thermodynamics*, 2nd ed., Wiley, New York (1989).

Savage, P. E., S. Gopalan, T. I. Mizan, C. J. Martino, and E. E. Brock, "Reactions at Supercritical Conditions: Fundamentals and Applications," *AIChE J.*, **41**(7), 1723 (1995).

Trapnell, B. M. W., *Chemisorption*, Butterworths, London (1955).

Tremaine, P. R., and J. C. LeBlanc, "The Solubility of Magnetite and the Hydrolysis and Oxidation of Fe^{2+} in Water to 300 C," *J. Solution Chem.*, **9**(6), 415 (1980a).

Tremaine, P. R., and J. C. LeBlanc, "The Solubility of Nickel Oxide and Hydrolysis of Ni^{2+} in Water to 573 K," *J. Chem. Thermody.*, **12**, 521 (1980b).

Zecchina, A., S. Coluccia, E. Guglielminotti, and G. Ghiotti, "An Infrared Study of Surface Properties of α-Chromia: I. Preparation and Adsorption of Water, Heavy Water; and Carbon Monoxide," *J. Phys. Chem.*, **75**(18), 2774 (1971a).

Zecchina, A., S. Coluccia, E. Guglielminotti, and G. Ghiotti, "An Infrared Study of Surface Properties of α-Chromia: II. Oxygen Chemisorption, *J. Phys. Chem.*, **75**(18), 2783 (1971b).

Manuscript received July 31, 1995, and revision received Nov. 2, 1995.